

PHARMACEUTICAL NANOTECHNOLOGY

Fabrication of Paclitaxel Nanocrystals by Femtosecond Laser Ablation and Fragmentation

SUKHDEEP KENTH,¹ JEAN-PHILIPPE SYLVESTRE,² KATHRIN FUHRMANN,³ MICHEL MEUNIER,² JEAN-CHRISTOPHE LEROUX^{1,3}

¹Canada Research Chair in Drug Delivery, Faculty of Pharmacy, Université de Montréal, Montréal, Quebec, Canada

²Canada Research Chair in Laser Micro/Nano-engineering of Materials, Laser Processing and Plasmonics Laboratories, Department of Engineering Physics, École Polytechnique de Montréal, Montréal, Quebec, Canada

³Institute of Pharmaceutical Sciences, Department of Chemistry and Applied Biosciences, ETH Zürich, Zürich, Switzerland

Received 15 March 2010; revised 4 June 2010; accepted 4 August 2010

Published online 31 August 2010 in Wiley Online Library (wileyonlinelibrary.com). DOI 10.1002/jps.22335

ABSTRACT: Nanonization, which involves formulating the drug powder as nanometer-sized particles, is a known method to improve drug absorption and allow the intravenous administration of insoluble drugs. This study investigated a novel femtosecond (fs) laser technique for the fabrication of nanocrystals in aqueous solution of the insoluble model drug paclitaxel. Two distinct methods of this technology, ablation and fragmentation, were investigated and the influence of laser power, focusing position and treatment time on the particle size, drug concentration, and degradation was studied. The colloidal suspensions were characterized with respect to size, chemical composition, morphology, and polymorphic state. Optimal laser fragmentation conditions generated uniformly sized paclitaxel nanoparticles (<500 nm) with quantifiable degradation, while ablation followed by fragmentation was associated with a larger polydispersity. Laser treatment at higher powers produced smaller particles with larger amount of degradation. The crystalline morphology of the drug was retained upon nanonization, but the anhydrous crystals were converted to a hydrated form, a phenomenon also observed during bead milling. These findings suggest that drug nanocrystals can be produced with fs laser technology using very little drug quantities, which may be an asset for preclinical evaluation of new drug candidates. © 2010 Wiley-Liss, Inc. and the American Pharmacists Association J Pharm Sci 100:1022–1030, 2011

Keywords: nanotechnology; nanoparticles; particle size; paclitaxel; femtosecond laser; pre-clinical development; preformulation; cancer; physicochemical

INTRODUCTION

Over the recent years, drug design has explored and developed new chemical species resulting in more complex molecules with higher hydrophobicities. It is estimated that 40% or more of active substances being identified through combinatorial screening programs are poorly water soluble. Consequently, formulation of these drugs presents a major challenge to their clinical development.¹ As a result of their very low aqueous solubility, such drugs cannot be injected and/or often have low

bioavailability. Classical methods to increase the solubility include micellar solubilization, complexation (e.g., cyclodextrins), and use of organic solvents. However, these approaches are limited in their success.² A common strategy to enhance the dissolution rate of a drug is to decrease the particle size and hence increase the surface area of the drug powder. Nanonization, which involves formulating the drug powder as nanometer-sized particles, was developed to further improve drug absorption and allow the intravenous administration of insoluble drugs.³ There exist several methods to produce drug nanoparticles, of which at least two are used commercially: NanoCrystal[®] technology (Elan), based on a mechanical process of wet milling, and DissoCube[®] (SkyePharma), a high-pressure homogenization technique.^{2,4} Concerns are often raised regarding the quality and durability of the milling media used in manufacturing and possible

Additional Supporting Information may be found in the online version of this article. Supporting Information

Correspondence to: Jean-Christophe Leroux (Telephone: +41-44 633-73-10; Fax: +41-44-633-13-11; E-mail: jleroux@ethz.ch)

Journal of Pharmaceutical Sciences, Vol. 100, 1022–1030 (2011)

© 2010 Wiley-Liss, Inc. and the American Pharmacists Association

contamination of the product following erosion of the grinding material. Disadvantages of the latter method are that before preparing the dispersion, the drug needs to be micronized and changes in drug crystallinity have also been reported.²

Laser techniques have been used extensively for the production of metal (e.g., Au, Ag) and organic [e.g., vanadyl phthalocyanine (VOPc)] nanoparticles.^{5,6} These methods consist of either irradiating a solid target or a stirred suspension yielding to the breaking of macroparticles into nanoparticles.^{5,7} The production of nanoparticles using laser irradiation has proved to be a simple and versatile technique in which stable and contaminant-free nanoparticles are generated⁸ and thus toxicity problems associated with conventional methods of nanofabrication are avoided.⁵ Previously, nanosecond (ns) laser fragmentation method, in which a laser beam is focused into a stirring organic microsuspension, was developed for the preparation of VOPc and quinadron nanoparticles in suspension.^{6,9} More recently, this technique was explored to fabricate colloidal fullerene (C₆₀) nanoparticles and 3,4,9,10-perylenetetracarboxylicdianhydride (PTCDA) nanoparticles.^{6,10} These studies reported very little information both on the degradation and on the polymorphic transformation of the organic material upon laser fragmentation. Furthermore, these fabricated organic nanoparticles were for applications in cosmetics and optical/electronic devices⁶ and not for drug delivery. Only one group has reported the production of drug (indomethacin) nanoparticles by ns Nd:YAG laser technique, whereby laser ablation (irradiation of a solid target) was performed with an ns pulsed laser in a dry environment (i.e., the absence of a dispersing medium and a stabilizing colloid/surfactant).⁷ Some changes in the crystallinity of indomethacin were observed.

Alternatively, femtosecond (fs) laser technology is more favorable than the ns laser, because fs pulses offer the advantage of irradiating materials with less energy, thus limiting the possible alteration of the ablated drugs nanocrystals. Therefore, the fs laser irradiation in liquid could prove to be efficient and nondestructive for the production of drug nanocrystals. In addition, performing fs laser ablation in an appropriate aqueous medium will generate sterically stabilized particles in a dispersed (nonagglomerated) state. Not only has the fs laser recently proven to be effective to produce fine inorganic nanoparticles with narrow size distribution^{5,11} but has also been shown to fabricate smaller sized organic particles than the ns laser strategy.¹²

Previously described to fabricate gold nanoparticles,¹¹ the novel fs laser technology investigated here is based upon two distinct methods: ablation and fragmentation. The first consists of a laser beam focused onto a solid target immersed in

a liquid, resulting in the ablation of the material and dispersion of the product into the liquid. The subsequent colloidal suspension is then subjected to a second laser treatment (fragmentation) in order to refine particle size, resulting in smaller and narrower size-distributed nanoparticles.⁵ The present work thoroughly explores the fabrication of drug nanocrystals by fs laser ablation/fragmentation in aqueous media, with a comprehensive characterization and degradation examination of produced nanocrystals, and describes the influence of process parameters on the physicochemical characteristics of the drug. The poorly soluble model drug used is paclitaxel (Fig. S1), an anticancer agent isolated from the bark of *Taxus brevifolia*. Paclitaxel is generally dissolved in a vehicle of 50:50 Cremophor EL and ethanol blend, which is further diluted with normal saline before intravenous administration. The disadvantage of this formulation (Taxol[®]) is that Cremophor EL causes severe adverse reactions (e.g., hypertension reactions, nephrotoxicity, and neurotoxicity).^{13,14} These side effects can be substantially alleviated by formulating paclitaxel as a nanoparticulate formulation.¹⁵

Experimental

Materials

Poloxamer 188 was supplied by BASF (Mississauga, Ontario, Canada). Anhydrous paclitaxel (purity 99.2%) was purchased from Bioxel Pharma (Sainte-Foy, Quebec, Canada). Dihydrate paclitaxel was purchased from Guanyu Bio-Technology Co. (Xi'an, Shaanxi, China). Diphenylhydantoin (DPH), which served as an internal standard, and Baccatin III were obtained from Sigma-Aldrich (Oakville, Ontario, Canada). 7-Epipaclitaxel, 7-epi-10-deacetylpaclitaxel, and 10-deacetylpaclitaxel were purchased from 21CEC PX Pharm Ltd. (Eastbourne, East Sussex, UK). Deionized water (18.2 MΩ·cm) was generated using Millipore Milli-Q system (Bedford, Massachusetts) and all other reagents were of analytical or high-performance liquid chromatography (HPLC) grade.

Methods

Preparation of Paclitaxel Tablet and Suspension

Pure drug (anhydrous) tablets without excipients were prepared in a hydraulic press using 4-mm diameter punches. The applied pressure was 3.9×10^8 N/m² for 25 s. Paclitaxel suspensions (200 μg/mL) were prepared by adding paclitaxel (anhydrous) powder to freshly prepared poloxamer 188 (8 mg/mL) aqueous solution, a regulatory accepted stabilizer for intravenous administration.¹⁶ The suspension was

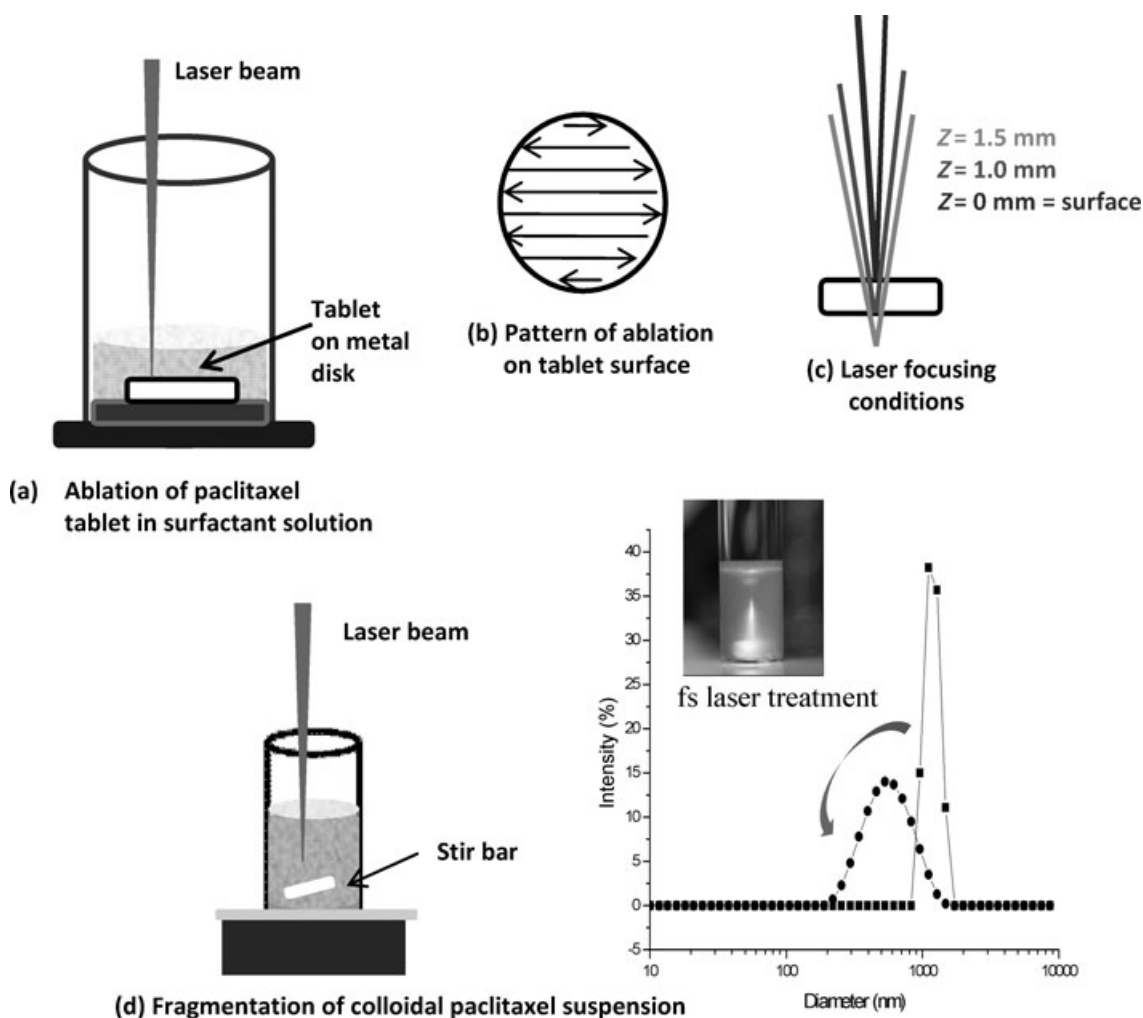


Figure 1. Representation of fs laser ablation (a–c) and fragmentation (d) methods.

sonicated (10 min) and stirred vigorously for several hours to obtain a homogenous sample.

Femtosecond Laser Treatment

Femtosecond laser radiation was used to ablate a solid paclitaxel tablet placed at the bottom of a 10-mL glass beaker filled with 3.5 mL of poloxamer 188 solution (8 mg/mL) (Fig. 1a). The tablet was held in place within a hole having the size of the tablet performed in a metal disk. The experiments were carried out using a Hurricane, Spectra Physics Ti:sapphire laser (Newport Corporation, Mountain View, California), providing 120 fs pulses centered at 800 nm with a repetition rate of 1 kHz. The beam was focused by an objective with the focal length of 7.5 cm. The focal spot was moved in a zig-zag like pattern (0.5 mm/s) using a motorized stage to obtain identical surface conditions during the laser ablation process (Fig. 1b). Different parameters were varied, such as the power of ablation (25–400 mW), treatment time (10–60 min), and different focusing conditions, that is, z positions of 0, 1, and 1.5 mm

(Fig. 1c). Further size refinement was carried out using laser fragmentation of the produced drug nanocrystal dispersion. The drug suspension was transferred into another glass vial and the laser was focused in the middle of the stirred solution (500 rpm) for 60 min (Fig. 1d). The average laser power was varied from 25 to 400 mW.

Alternatively, single-step fragmentation (no prior ablation) was conducted using prepared paclitaxel suspension (200 $\mu\text{g/mL}$). Paclitaxel suspension (2.5 mL) was added to a small cuvette with a stir bar, and fragmentation (500 rpm) for 60 min at powers ranging from 50 to 400 mW (Fig. 1d).

Paclitaxel Assay

The amount of paclitaxel and degradation products in suspension after laser treatments was evaluated by HPLC. The sample suspension was first mixed with equal volume of acetonitrile to dissolve the particles. After vortexing, the internal standard, DPH (50 $\mu\text{g/mL}$), was added, and the sample was filtered through 0.2- μm nylon membrane. Injection volume was 70 μL .

HPLC was performed using a Waters HPLC system (Waters, Mississauga, Ontario, Canada) with a C18 column (3.5×16 mm, $d_p = 3$ μ m). The elution was performed using an isocratic mix of water and acetonitrile 3:2 (v/v) for 26 min, continuing with a gradient acetonitrile and mix 0:100 to 43:57 within 21 min, at an elution rate of 1.2 mL/min. UV detection was set at 227 nm and column temperature was maintained at 35°C. Before sampling, calibration curves for paclitaxel and all four degradation products (baccatin III, 7-epipaclitaxel, 7-epi-10-deacetylpaclitaxel, and 10-deacetylpaclitaxel) were established (linearity range = 0.3–200 μ g/mL). The content of paclitaxel and degradation products (μ g/mL) was calculated using their respective calibration curves. The percentage degradation corresponded to the sum of degradation products (μ g/mL) divided by the sum of paclitaxel and total degradation products $\times 100$.

Particle Size Analysis and Zeta Potential Measurements

The size of nanocrystals was determined by dynamic light scattering, using Malvern Zetasizer NanoSeries, with a detection angle of 173° (Malvern, Worcestershire, UK). Each measurement was performed in triplicate on undiluted suspension in low-volume disposable sizing cuvette at 25°C. The CONTIN program was used to extract size distributions from the autocorrelation functions. The zeta potential of the nanocrystals was measured by electrophoretic mobility using Zetasizer NanoSeries; samples were prepared by mixing 400 μ L of nanocrystal suspension with 500 μ L of Milli-Q water and 100 μ L of saline (0.9% NaCl in water). Each measurement was performed in triplicate in disposable zeta cells at 25°C.

Scanning Electron Microscopy

Morphological evaluation of the optimal paclitaxel nanocrystals was conducted by scanning electron microscopy (SEM). The nanosuspension fabricated by fragmentation was cleaned by centrifugation to remove the excess surfactant. A drop of suspension was placed on a silicon substrate and dried overnight in a desiccator under vacuum. The sample was observed with a FE-MEB S-4700 field-emission scanning electron microscope (Hitachi, Tokyo, Japan). Paclitaxel control sample (water-exposed nonfragmented) was prepared by adding pure paclitaxel drug powder to poloxamer 188 solution, sonicated (10 min) and stirred for several hours, but not subjected to laser treatment.

Thermal Analysis

For thermogravimetric analysis (TGA) and differential scanning calorimetry (DSC), the fragmented nanocrystal and control samples were prepared without poloxamer 188, in order to avoid signal interference from the polymer, which degraded before the

melting point of paclitaxel. TGA of the anhydrous paclitaxel, dihydrate paclitaxel, fragmented nanocrystals, and water-exposed nonfragmented drug was performed with a TA Instruments TGA 2950 system (TA Instruments, New Castle, Delaware). Approximately 3 mg of the paclitaxel sample was weighed in a platinum pan and heated to 700°C at a rate of 10°C/min under nitrogen purge. Thermal properties were obtained by a DSC TA Instruments DSC Q200 system (TA Instruments). Samples of 2 to 3 mg were placed and sealed in Tzero pinhole pans and analyzed at a heating rate of 50°C/min. High heating rate was used to avoid decomposition of the drug in the DSC furnace.

Spectroscopic Analysis

Paclitaxel samples were analyzed by Fourier transform infrared spectroscopy (FTIR) for chemical composition and by X-ray diffractometry (XRD) for crystallinity. Prior to FTIR and XRD analyses, the control sample (raw paclitaxel suspended in poloxamer 188 by sonication and stirring) and the laser-fragmented nanocrystals were both cleaned by ultracentrifugation and then lyophilized. First, the samples were centrifuged for 15 min at $10,600 \times g$. The sedimented particles were washed with Milli-Q water, resuspended and centrifuged twice more to remove the residual poloxamer 188, and then lyophilized for 72 h. FTIR and XRD spectra were obtained for the lyophilized nanocrystals and control sample (nonfragmented), the raw anhydrous, and dihydrate paclitaxel samples. FTIR analysis, with a resolution of 4 cm^{-1} , was performed with a Bio-Rad Excalibur Series spectrometer, FTS3000 (Bio-Rad Laboratories, Randolph, Massachusetts) using the potassium bromide (KBr) pellet technique. Each 150-mg pellet contained 2 mg of the paclitaxel sample. XRD spectra were obtained with an X'Pert X-ray PANalytical diffractometer (PANalytical Inc., Montréal, Quebec, Canada) using the grazing angle method in which the X-ray source was fixed at $\omega = 2^\circ$. Samples of 10 to 15 mg were used. The x-ray source was Cu K α (50 kV 40 mA). The 2θ range scanned was 5° to 50° at a rate of 0.02°/s.

RESULTS AND DISCUSSION

In the first part of this work, fs laser ablation followed by subsequent fragmentation was explored. The ablation process was investigated as a function of power (25–400 mW), focusing position ($z = 0, 1, \text{ and } 1.5$ mm), and ablation time (20–60 min). Upon completion of the ablation process, the suspension was collected, paclitaxel particles were dissolved in acetonitrile, and analyzed by HPLC for paclitaxel concentration and degradation products. Figure 2a shows the concentration of paclitaxel particles produced after ablation (for 20 min) as a function of laser power for three focusing positions. It was observed that as z increased

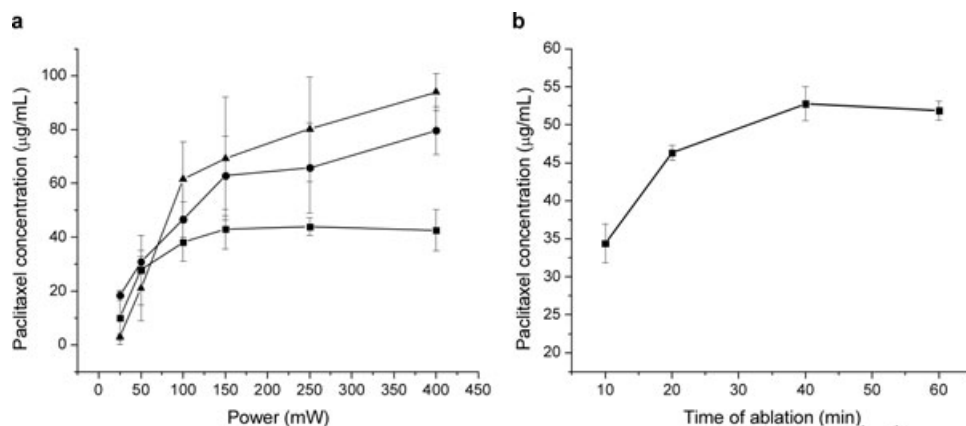


Figure 2. (a) Paclitaxel concentration of the suspensions prepared by fs laser ablation at focusing positions of $z = 0$ mm (squares), 1 mm (circles) and 1.5 mm (triangles), at power ranging from 25 to 400 mW, ablation time = 20 min. Mean \pm SD ($n = 3$). (b) Paclitaxel concentration of the colloidal suspensions prepared by fs laser ablation at focusing positions $z = 1$, 150 mW, and time ranging from 10 to 60 min. Mean \pm SD ($n = 3$).

from 0 to 1.5 mm, more paclitaxel was ablated from 100 mW. A plausible explanation for this observation is that a variation of the focusing condition from $z = 0$ to 1.5 mm corresponds to an increase in the surface area of the laser irradiation spot at the tablet surface (Fig. 1c). At z positions of 1 and 1.5 mm, increasing the power from 25 to 400 mW resulted in a higher concentration of the suspended paclitaxel particles. In all cases, degradation was relatively low but greater at $z = 1.5$ (ca. 2%). The size of the particles was independent of the power because particles ranging from 800 to 3000 nm were observed at all powers (data not shown). The degradation was not significantly different as function of power for a given z position. As ablation at $z = 1.5$ mm generated the largest degradation, subsequent experiments were carried out at $z = 1$ mm (Table 1). The effect of ablating time was then assessed at a power of 150 mW. As illustrated in Figure 2b, the amount of paclitaxel particles produced increased as a function of exposure time. After 20 min, the paclitaxel concentration remained relatively constant as a function of time, reaching a plateau from 40 to 60 min (~ 50 µg/mL). This phenomenon suggests that after 20-min ablation, the suspension

became relatively turbid, causing the laser beam to be scattered, thereby reducing the energy available to ablate the tablet and decreasing the ablation efficiency. Ablation for more than 20 min also generated more degradation (data not shown). The optimal ablation condition was selected as: $z = 1$ mm, treatment time of 20 min, and power of 150 mW. Next, a stock suspension prepared via optimal ablation was subjected to fragmentation from 25 to 400 mW. This second laser treatment did refine the mean diameter of the particles; particles as small as 50 nm were obtained; however, the particle size distribution remained considerably large (Table 2). Degradation also increased with laser power, reaching levels of nearly 10% at 250 and 400 mW. This was accompanied by a decrease in the concentration of paclitaxel. The zeta potential was almost neutral and did not change with fragmentation conditions.

As the overall efficiency of the two-step ablation/fragmentation process was limited by the amount of drug ablated in the initial step, an alternative strategy based upon fragmentation alone was explored. A paclitaxel suspension (~ 200 µg/mL) was prepared directly by adding the drug powder to the poloxamer 188 solution. The suspension was fragmented at powers ranging from 50 to 400 mW, and size and degradation were measured (Table 3). As the power increased, smaller particles with reasonable polydispersities (PDI ≈ 0.3)¹⁷ were obtained; however, higher degradation was observed (up to 23% at 400 mW). This trend in particle size was reported in other studies involved in the production of C₆₀ and VOPc nanoparticles using a ns laser fragmentation method,^{6,9} suggesting that higher laser power provides greater energy to fragment particles, thus smaller nanocrystals are obtained. This single-step fragmentation process yielded a smaller size

Table 1. Degradation of the Paclitaxel Colloidal Suspensions Generated by Ablation at Three Focusing Conditions*

Power (mW)	Degradation (%)		
	$z = 0$ mm	$z = 1$ mm	$z = 1.5$ mm
25	0.7 \pm 1	0.3 \pm 0.2	1.8 \pm 1.7
50	0.3 \pm 0.4	0.5 \pm 0.3	2.9 \pm 1.9
100	0.5 \pm 0.5	1.0 \pm 0.5	2.2 \pm 0.7
150	0.8 \pm 0.4	0.8 \pm 0.1	2.3 \pm 1.3
250	0.8 \pm 0.3	1.1 \pm 0.2	2.8 \pm 1.1
400	0.8 \pm 0.4	1.8 \pm 0.7	2.1 \pm 0.5

*Values given are mean \pm SD ($n = 3$).

Table 2. Concentration of Paclitaxel (PTX), Chemical Degradation, Size Distribution, and Surface Charge of PTX Suspensions Prepared by Two-Step Femtosecond Laser Ablation and Fragmentation*

Power (mW)	[PTX] ($\mu\text{g/mL}$)	Degradation (%)	Size (nm)	Polydispersity	Zeta potential (mV)
0	37.3 ± 3	1.6 ± 1	2700 ± 800	0.9 ± 0.2	-6.0 ± 3.0
25	34.5 ± 4	4.0 ± 1	2000 ± 500	0.7 ± 0.2	-5.6 ± 0.4
50	32.3 ± 3	3.3 ± 2	2200 ± 600	0.9 ± 0.1	-6.8 ± 0.5
100	33.2 ± 2	2.8 ± 1	1500 ± 450	0.7 ± 0.3	-6.2 ± 0.3
150	30.8 ± 1	3.8 ± 2	1100 ± 400	0.3 ± 0.2	-4.4 ± 0.2
250	14.1 ± 2	9.7 ± 1	300 ± 100	0.6 ± 0.2	-5.8 ± 0.9
400	10.3 ± 1	8.0 ± 3	50 ± 15	0.7 ± 0.2	-1.0 ± 0.6

*Values given are mean \pm SD ($n = 3$).

Table 3. Chemical Degradation and Size Distribution of Paclitaxel Particles Obtained by Fragmentation (60 min)*

Power (mW)	Size (nm)	Polydispersity	Degradation (%)
50	3000 ± 160	0.29 ± 0.20	1.2 ± 0.14
100	1100 ± 70	0.34 ± 0.07	8.3 ± 0.41
150	800 ± 30	0.32 ± 0.05	12.6 ± 1.3
250	600 ± 50	0.31 ± 0.04	17.1 ± 1.7
400	400 ± 60	0.29 ± 0.07	23.1 ± 2.0

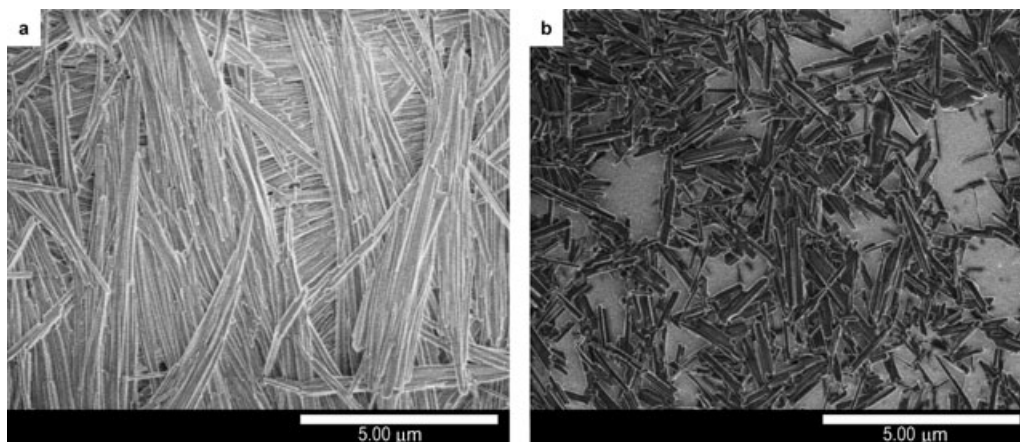
*Values given are mean \pm SD ($n = 3$).

distribution than the ablation/fragmentation method. The morphology assessment by SEM confirmed that significant nanonization occurred during laser fragmentation. The original needle-like shape was retained upon fragmentation at 400 mW for 60 min, and size was reduced from micro- to nanoparticles (Fig. 3). In previous studies, it was demonstrated that laser irradiation of VOPc microcrystals dispersed in solvent changed the morphology of the initial crystals.⁹ Such a morphological change was not observed when paclitaxel was fragmented using the fs laser technique.

Following the size and degradation examination of the paclitaxel particles, further characterization was carried out to evaluate the state of the drug upon laser fragmentation. The fs laser generated nanoparticles were compared with anhydrous paclitaxel,

dihydrate paclitaxel, and a nonfragmented water exposed sample, which was fabricated by suspending the anhydrous drug in the aqueous solution followed by lyophilization. FTIR spectroscopy was used to characterize the hydration state of the various paclitaxel samples (Fig. 4). The peak shapes of anhydrous paclitaxel and the water-exposed, nonfragmented paclitaxel were similar at 3500 and 1650 cm^{-1} . At these wavenumbers, the dihydrate paclitaxel and the laser-fragmented sample displayed broadened and less defined peaks, suggesting hydration of the drug upon laser fragmentation. A general trend was observed: the peaks became less defined (e.g., loss of doublet peak around 1650 cm^{-1}) and broadened as the sample becomes more hydrated. This phenomenon has been reported before.¹⁸

As expected, DSC analysis showed that the anhydrous paclitaxel exhibited a sharp melting point at ca. 225°C.¹⁹ The water-exposed paclitaxel non-fragmented sample also displayed this melting endotherm, indicating presence of anhydrous paclitaxel. However, the TGA analysis displayed a mass drop of 2.2%, suggesting presence of water in the water-exposed, nonfragmented paclitaxel sample (Fig. S2). Dihydrate paclitaxel exhibited a broad endotherm from approximately 50°C to 125°C corresponding to water evaporation.^{19,20} A similar, but less broad,

**Figure 3.** Scanning electron micrographs of (a) water-exposed, nonfragmented paclitaxel and (b) laser-fragmented paclitaxel nanocrystals (400 mW, 60 min).

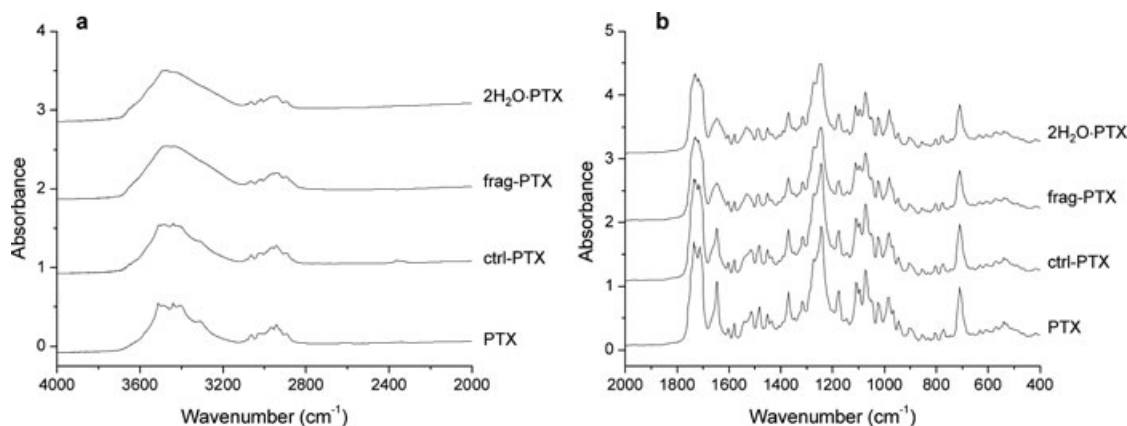


Figure 4. FTIR spectra of dihydrate paclitaxel ($2\text{H}_2\text{O}\cdot\text{PTX}$), laser-fragmented (400 mW, 60 min) nanocrystals (frag-PTX), water-exposed, nonfragmented paclitaxel (ctrl-PTX), and anhydrous paclitaxel (PTX).

endotherm was observed in the fragmented sample, indicating that this sample displayed a hydrated nature. In addition, a significant endothermic peak at 170°C , reported as a solid-solid transition by Liggins et al.,¹⁹ was observed in the dihydrate paclitaxel and to a lesser extent in the laser-fragmented sample. This endotherm is significant of dehydrated dihydrate paclitaxel converting to a semicrystalline form. The distinct melting endotherm characteristic of anhydrous paclitaxel (225°C) was also observed in the dihydrate paclitaxel sample but was not seen in the laser-fragmented sample (Fig. 5). DSC analysis showed the degradation of the fragmented sample at temperatures above 220°C , this correlated with the TGA analysis, which demonstrated that degradation occurred at a lower temperature than the other pa-

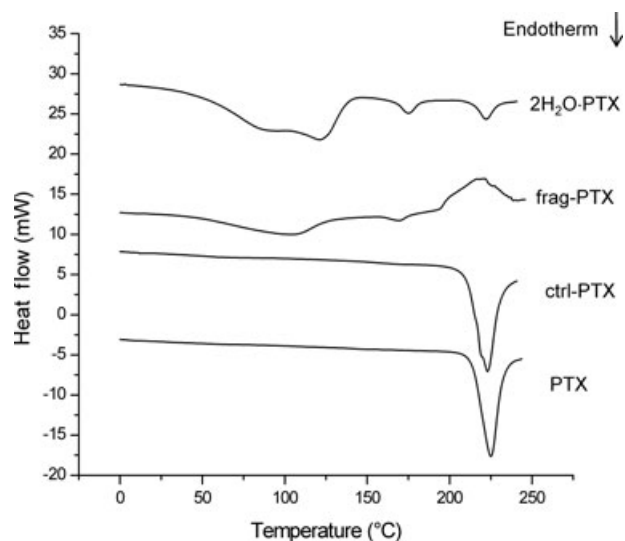


Figure 5. DSC thermograph of anhydrous paclitaxel (PTX), water-exposed, nonfragmented paclitaxel (ctrl-PTX), laser-fragmented (400 mW, 60 min) nanocrystals (frag-PTX), and dihydrate paclitaxel ($2\text{H}_2\text{O}\cdot\text{PTX}$).

clitaxel samples (Fig. S2). This could be explained by the presence of impurities (degradation products) or the nanosize of the crystals (Fig. 5).

To obtain more insight into the polymorphic state of the drug nanoparticles generated by fs laser fragmentation, XRD analysis was performed on the drug samples (Fig. 6, Table S1). Anhydrous paclitaxel exhibited characteristic XRD peaks at $2\theta = 5.6^\circ, 9.1^\circ, 10.4^\circ, 12.7^\circ,$ and 21.1° .¹⁹ Anhydrous and dihydrate paclitaxel demonstrated different XRD patterns, suggesting that a polymorphic transformation occurred upon hydration of anhydrous paclitaxel.^{18,19} Five new peaks (6.2, 9.8, 11.2, 13.3, and 16.7°), which were all absent in the anhydrous paclitaxel, appeared in the water-exposed control, laser-fragmented, and dihydrate samples, thus suggesting partial hydration of paclitaxel. As the anhydrous paclitaxel was suspended in water, it became slightly hydrated as evidenced by the apparition of peaks characteristic of the

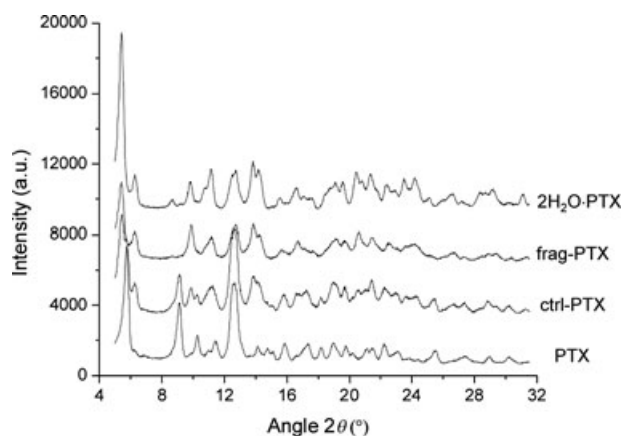


Figure 6. XRD analysis of dihydrate paclitaxel ($2\text{H}_2\text{O}\cdot\text{PTX}$), laser-fragmented (400 mW, 60 min) nanocrystals (frag-PTX), water-exposed, nonfragmented paclitaxel (ctrl-PTX), and anhydrous paclitaxel (PTX).

dihydrate form. As fragmentation was performed, the hydration of the drug augmented and thus displayed similar XRD patterns to dihydrate paclitaxel. The hydration of the paclitaxel was independent of the laser technique. It has been previously demonstrated that anhydrous paclitaxel suspended in water over a period of time generates a hydrated state of the drug.¹⁹ Moreover, the paclitaxel suspension (particle size = 700–800 nm) prepared by bead milling displayed similar features to the laser-fragmented sample, suggesting that nanonization of paclitaxel in water transforms anhydrous drug into the hydrated state (Fig. 6 and Fig. S3).

By compiling the calorimetry and spectroscopy results, it appears that the anhydrous drug underwent crystalline change into dihydrate form after fs laser treatment in water. This polymorphic transformation of anhydrous paclitaxel also occurs in another nanonization technique performed in water (bead milling), therefore is not exclusive to the fs laser technology (Fig. S3). Therefore, the polymorphic transformation of paclitaxel is most likely due to the nature of the drug and not due to the fs laser technology. The slight differences between the laser fragmented and the dihydrate samples may be due to the presence of degradation products or small size of the nanocrystals. These two paclitaxel forms both exhibit needle-shaped crystal structure.¹⁹ In previous work reporting the laser fragmentation of organic suspensions, quantitative degradation studies were not performed.^{10,21} Sugiyama et al.²¹ assessed the photoproducts of C₆₀ by ¹³C NMR. They revealed that no appreciable photoproduct was formed under specific ns laser irradiation conditions, although decomposition of C₆₀ was induced at a higher fluence. Hopley et al.¹⁰ used the similar ns pulsed laser technique to fabricate PTCDA nanoparticles. By-products of PTCDA were identified but no quantitative degradation study was conducted. In the present work, nanoparticles of a complex drug molecule were prepared by fs laser method and the production of degradation products was monitored. The fs laser treatment was previously shown to generate smaller particles than by ns laser.¹² However, as can be seen in Tables 2 and 3, the fabrication of particles of less than 1000 nm was associated with significant degradation of paclitaxel. The latter is a labile molecule^{22,23} and therefore it can be expected that chemically less complex and more stable drugs would be better suited for nanonization by fs laser treatment. To decrease the degradation process, fragmentation was performed under an inert atmosphere (argon) in the presence of antioxidants (L-cysteine) or with other stabilizing agents (polysorbate 80, polyvinylpyrrolidone). However, these approaches proved unsuccessful (data not shown). Therefore, the degradation was not related to the presence of dis-

solved oxygen in the suspension but rather may be due to the high local temperatures generated at the focal point during laser treatment.

The fs laser technology presented here may be valuable in the preclinical development. Indeed, in the preformulation and late discovery stage, compound availability is scarce and thus examining numerous formulation approaches is difficult.^{24,25} Using the fs laser technology on minute amounts of drug (microgram–milligram) to fabricate nanoparticles may be advantageous as an *in vivo* screening approach. If the nanocrystal formulation appears to be promising (i.e., displays good bioavailability), then more conventional techniques could be applied for the production of greater amounts of nanocrystals without degradation. However, sensitive drugs, such as paclitaxel, are perhaps not the best drug candidates for this nanonization technique in the preclinical context, and in particular in pharmacodynamic studies, as the presence of significant levels of degradation products could mislead the screening process. Nevertheless, work in progress for other hydrophobic drugs, such as megestrol acetate, suggests that fs laser fragmentation may be an alternative route for the production of nanoparticles of other poorly water soluble and less sensitive drugs.²⁶ Finally, another current limitation of the fs technique as presented here is that the efficiency of the process is limited by the increase in turbidity of the suspension as more particles are produced. However, this problem could be easily solved by implementing a continuous flow system, which may also eventually lead to lower degradation of the drug.

CONCLUSIONS

In this work, fs laser irradiation was explored for the fabrication of paclitaxel nanocrystals. Narrowly dispersed paclitaxel nanoparticles of approximately 400 nm were obtained by single-step fragmentation. However, they were associated with significant degradation. The polymorphic transformation of paclitaxel into the dihydrate state is not associated with the fs laser conditions but rather is characteristic of any nanonization method performed in water. Although several studies have reported the use of laser technology for the development of organic nanoparticles, this is the first investigation where the fs laser fragmentation technique is used for the fabrication of paclitaxel nanocrystals in aqueous medium and in which the nanocrystals have been fully characterized.

Using the fs laser technique as a preclinical screening tool, this work may translate into successful future avenues for the production of drug nanocrystals for an array of pathologies including cancer and infectious diseases.

ACKNOWLEDGMENTS

Financial support was provided by the Natural Sciences and Engineering Research Council of Canada (NSERC), the Canadian Institutes of Health Research (CIHR), the Groupe de Recherche Universitaire sur le Médicament (GRUM), and Fonds de la recherche en santé du Québec (FRSQ). Special thanks to Dr. Marc Gauthier for proofreading the text.

REFERENCES

- Rabinow BE. 2004. Nanosuspensions in drug delivery. *Nat Rev Drug Discov* 3:785–796.
- Muller RH, Jacobs C, Kayser O. 2001. Nanosuspensions as particulate drug formulations in therapy. Rationale for development and what we can expect for the future. *Adv Drug Deliv Rev* 47:3–19.
- Merisko-Liversidge E, Liversidge GG, Cooper ER. 2003. Nanosizing: A formulation approach for poorly-water-soluble compounds. *Eur J Pharm Sci* 18:113–120.
- Keck CM, Muller RH. 2006. Drug nanocrystals of poorly soluble drugs produced by high pressure homogenisation. *Eur J Pharm Biopharm* 62:3–16.
- Besner S, Kabashin A, Winnik F, Meunier M. 2008. Ultrafast laser based “green” synthesis of non-toxic nanoparticles in aqueous solutions. *Appl Phys A: Mater Sci Process* 93:955–959.
- Asahi T, Sugiyama T, Masuhara H. 2008. Laser fabrication and spectroscopy of organic nanoparticles. *Acc Chem Res* 41:1790–1798.
- Nagare S, Senna M. 2004. Reagglomeration mechanism of drug nanoparticles by pulsed laser deposition. *Solid State Ionics* 172:243–247.
- Sylvestre JP, Kabashin AV, Sacher E, Meunier M. 2005. Femtosecond laser ablation of gold in water: Influence of the laser-produced plasma on the nanoparticle size distribution. *Appl Phys A: Mater Sci Process* 80:753–758.
- Tamaki Y, Asahi T, Masuhara H. 2002. Nanoparticle formation of vanadyl phthalocyanine by laser ablation of its crystalline powder in a poor solvent. *J Phys Chem A* 106:2135–2139.
- Hobley JN, Kajimoto T, Kasuya S, Hatanaka M, Fukumura K, Nishio H. 2007. Formation of 3,4,9,10-perylenetetracarboxylicdianhydride nanoparticles with perylene and polyene byproducts by 355 nm nanosecond pulsed laser ablation of microcrystal suspensions. *J Photochem Photobiol A: Chem* 189:105–113.
- Besner S, Kabashin AV, Meunier M. 2007. Two-step femtosecond laser ablation-based method for the synthesis of stable and ultra-pure gold nanoparticles in water. *Appl Phys A: Mater Sci Process* 88:269–272.
- Masuhara H, Sugiyama T, Asahi T. 2004. Formation of 10 nm-sized oxo(phthalocyaninato)vanadium(IV) particles by femtosecond laser ablation in water. *Chem Lett* 33:724–725.
- Dordunoo SK, Burt HM. 1996. Solubility and stability of taxol: Effects of buffers and cyclodextrins. *Int J Pharm* 133:191–201.
- Singla AK, Garg A, Aggarwal D. 2002. Paclitaxel and its formulations. *Int J Pharm* 235:179–192.
- Miele E, Tomao F, and Tomao S. 2009. Albumin-bound formulation of paclitaxel (Abraxane® ABI-007) in the treatment of breast cancer. *Int J Nanomed* 4:99–105.
- Muller RH, Keck CM. 2004. Challenges and solutions for the delivery of biotech drugs—a review of drug nanocrystal technology and lipid nanoparticles. *J Biotechnol* 113:151–170.
- Müller RH, Böhm BHL 1998. Nanosuspensions. In *Emulsions and nanosuspensions for the formulation of poorly soluble drugs*; Müller RH, Benita S, Böhm B, Eds. Stuttgart, Germany: Medpharm Scientific, pp 149–173.
- Pyo S-H, Cho JS, Choi HJ, Han BH. 2007. Preparation and dissolution profiles of the amorphous, dihydrated crystalline, and anhydrous crystalline forms of paclitaxel. *Dry Technol* 25:1759–1767.
- Liggins RT, Hunter WL, Burt HM. 1997. Solid-state characterization of paclitaxel. *J Pharm Sci* 86:1458–1463.
- Gi U-SM, Bumcham L, Jin-Hyun K. 2004. Preparation and characterization of paclitaxel from plant cell culture. *Korean J Chem Eng* 21:816–820.
- Sugiyama TR, Oh I, Asahi T, Masuhara H. 2009. Nanosecond laser preparation of C₆₀ aqueous nanocolloids. *J Photochem Photobiol A* 207:7–12.
- Jiaher T, Valentino JS. 2008. Degradation of paclitaxel and related compounds in aqueous solutions I: Epimerization. *J Pharm Sci* 97:1224–1235.
- Jiaher T, Valentino JS. 2009. Degradation of paclitaxel and related compounds in aqueous solutions III: Degradation under acidic pH conditions and overall kinetics. *J Pharm Sci* 99:1288–1298.
- Van Eerdenbrugh B, Van Den Mooter G, Augustijns P. 2008. Top-down production of drug nanocrystals: Nanosuspension stabilization, miniaturization and transformation into solid products. *Int J Pharm* 364:64–75.
- Van Eerdenbrugh BS, Froyen B, Van Humbeeck L, Martens J, Augustijns J, Van Den Mooter P. 2009. Downscaling drug nanosuspension production: Processing aspects and physicochemical characterization. *AAPS PharmSciTech* 10:44–53.
- Sylvestre JP, Kenth S, Lueling K, Meunier M, Leroux JC. 2009. Fabrication of dispersed megestrol acetate nanocrystals by laser fragmentation in water. In *2009 AAPS Annual Meeting and Exposition*, Los Angeles, California.